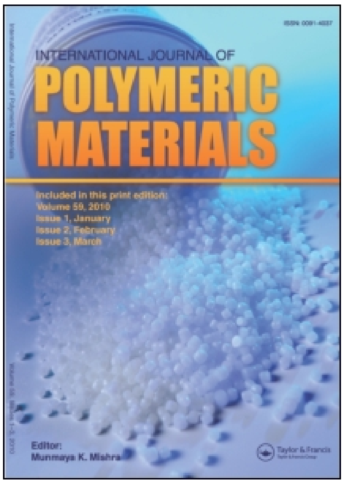

International Journal of Polymeric Materials
Publication details, including instructions for authors and subscription information:
http://www.informaworld.com/smpp/title~content=t713647664

Phase transitions in laterally substituted semi-rigid polyesters

M. Hess[a]; Ralf Woelke[a]; Byung-Wook Jo[b]
[a] Department of Physical Chemistry, Gerhard-Mercator-University, Duisburg, Germany [b] Department of Polymer Science and Engineering, Chosun University, KwangJu, Republic of Korea

To cite this Article Hess, M. , Woelke, Ralf and Jo, Byung-Wook(2003) 'Phase transitions in laterally substituted semi-rigid polyesters', International Journal of Polymeric Materials, 52: 4, 265 — 286
To link to this Article: DOI: 10.1080/00914030304920
URL: http://dx.doi.org/10.1080/00914030304920

International Journal of Polymeric Materials, 52: 265–286, 2003

0091-4037/03 $12.00 +.00
DOI: 10.1080/00914030390119451

PHASE TRANSITIONS IN LATERALLY SUBSTITUTED SEMI-RIGID POLYESTERS

M. Hess
Ralf Woelke
Department of Physical Chemistry,
Gerhard-Mercator-University, Duisburg, Germany

Byung-Wook Jo
Department of Polymer Science and Engineering,
Chosun University, KwangJu, Republic of Korea

The thermal transitions of a series of polyesters of the type poly[oxy(2,2′-dialkylpropane-1,3-diyl)carboxybisphenyl-4,4′-dicarbonyl] have been investigated using Differential Scanning Calorimetry. Crystallization as well as the glass-transition were studied with emphasis on the crystallization of the dimethylpropane derivative. The general tendency to show stable mesophases decreases with increasing length of the lateral alkyl substituents attached to the spacer. The glass transition is definitely not second order and more order parameters are required to describe the glassy state.

Keywords: phase transitions, structure-properties relations, semi-rigid polyesters

INTRODUCTION

Longitudinal polymer liquid crystals (PLCs), where the mesomorphic constituents of the polymer are localized within the main-chain, are of particular interest because of their potential as new high performance

Received 28 December 2000; in final form 4 January 2001.

This article is dedicated to Prof. Werner Borchard, Duisburg, on the occasion of his 65th birthday.

The authors express their thanks to the Korean Research Foundation (KOSEF) and the Deutscher Akademischer Austauschdienst (DAAD) for their financial support which has allowed M. Hess to work on this project at Chosun-University, KwangJu, South Korea, C. P. Lee for technical assistance, and K. Schwark for drawing the figures.

Address correspondence to M. Hess, Department of Physical Chemistry, Gerhard-Mercator-University, 47048 Duisburg, Germany.

materials [1]. The drawback of these polymers is a frequently observed low processability since the thermal transitions are often high so that degradation is supported and the solubility is unsatisfactory. Several strategies have been developed in the past to overcome these disadvantages without causing significant losses of the mechanical properties: flexible spacers connecting the mesogens, see *e.g.*, Lenz [2], bent or crankshaft-like comonomers, see *e.g.*, Calundann and Jaffe [3], rigid rod polymers with flexible side-chains, see *e.g.*, Ballauff and Schmidt [4]. Statistical mechanics [5–7] has been used to describe some of the structure-properties relations and different synthetic ideas have been developed to find new concepts. Depending on the type of modification they can affect to different extents molecular mobility, crystallization, packing and order of the molecules in the solid an in the molten state. We have been concentrating on the structure-properties effects of laterally branched semi-rigid polymers, different from the rigid-rod polymers with flexible side chains of another type as described above [4], since a couple of years [8–11]: in contrast to Ballauff, where side-chains were laterally attached to the rigid chain segment, the polymers we are interested in consist of rigid segments, such as carboxybisphenyl-4,4′ dicarbonyl-diyl or the corresponding terphenyl derivative. The rigid segments are connected by short, branched spacers like oxy-2,2′ dialkylpropane-1,3-diyl or oxy-2,3 dialkylbutane-1,4-diyl. We are interested in the effect of increasing lengths of the alkyl side-chain on physical properties of these polymers.

The biphenyl group is a weaker mesogen compared with the longer terphenyl, and the odd number of carbons of a propyl-spacer rather results in a bent chain while the even number of the carbons in a butyl group facilitate a more linear structure if there are corresponding interactions between the polymer chains. In the present paper we focus on structure-properties relations like crystallization and the analysis of the glassy transition in a series of poly[oxy(2,2′-dialkylpropane-1,3-diyl) carboxybisphenyl-4,4′-dicarbonyl]. These semi-rigid polymers also show an entirely different relaxation behaviour near the glass transition compared with the comparable (flexible) poly(methacrylesters), see Saiter et al. [12]. Optical, thermal and mechanical behaviour may impart these polymers a certain importance for application in sensors [13].

THEORY

The discussion of the behaviour of the polymers at the glass transition requires some theoretical background. The glassy state is a thermodynamic non-equilibrium situation and the glass transition is not a transition between two neighbouring states in equilibrium but a kinetically controlled process. The temperature dependence of the Gibbs Function G around the glass transition temperature resembles a continuous transition, a second order transition in the classification of Ehrenfest [14], and the Ehrenfest-equations derived thereof are only valid when there is equilibrium on both sides of the transition, that means if the substance can be described with only two degrees of freedom. Rehage [15] has checked this for PS. We have it now checked for the series of semi-rigid polymers.

For a continuous (second order) transition the second derivatives of the Gibbs Function show a discontinuity while there is a continuity of the total differentials along the transition curve and at the second order transition. Examples for continuous transitions are ^{4}He at the lambda point and the ferromagnetic transition at the Curie temperature.

From the continuity of G during a second order transition it follows that the specific volume υ and the specific entropy s are also continuous since they are equations of state so that for two phases' and "in thermodynamic equilibrium there is:

$$\mathrm{d}\upsilon'(\mathrm{T},\mathrm{p}) = \mathrm{d}\upsilon''(\mathrm{T},\mathrm{p}) \tag{1}$$

$$\mathrm{ds}'(\mathrm{T},\mathrm{p}) = \mathrm{ds}''(\mathrm{T},\mathrm{p}) \tag{2}$$

which yields:

$$-\kappa'\mathrm{dp} + \alpha'\mathrm{dT} = -\kappa''\mathrm{dp} + \alpha''\mathrm{dT} \tag{3}$$

and

$$-\alpha'\mathrm{dp} + (\mathrm{c}_\mathrm{p}'/\mathrm{T})\mathrm{dT} = -\alpha''\mathrm{dP} + (\mathrm{c}_\mathrm{p}''/\mathrm{T})\mathrm{dT} \tag{4}$$

with the definitions of the isothermal compressibility κ, the isobaric coefficient of expansion α, the heat capacity at constant pressure c_p and the specific volume υ and the specific entropy s the two Ehrenfest equations [14,15] can be derived:

$$\mathrm{dp}/\mathrm{dT} = \Delta\alpha/\Delta\kappa \tag{5}$$

and

$$\mathrm{dp}/\mathrm{dT} = \Delta\mathrm{c}_\mathrm{p}/(\mathrm{T}\Delta\alpha\upsilon_{\mathrm{trans}}) \tag{6}$$

or

$$\mathrm{T}(\Delta\alpha)^2/(\Delta\kappa\Delta\mathrm{c}_\mathrm{p}\upsilon_{\mathrm{trans}}) = 1 \tag{7}$$

Δ denotes the step in the value of the corresponding quantity just before and just after the transition. $\upsilon_{\mathrm{trans}}$ is the specific volume of the system at the transition temperature. A deviation of the behaviour of the glass transition from Eq. (7) means that there are more than one order parameters necessary to formally describe the glassy solidification [16].

MATERIALS AND METHODS

The synthesis of the polymers followed the general paths outlined by Stickford et al. [9]. The molar mass of the polymers was determined by size-exclusion chromatography coupled with a WYATT multi-angle-laser-light-scattering in THF at room temperature. The mass-average molar mass $\langle Mw \rangle$ of the polymers was about 13,700 g/mol (DP 1,1) 27,000 g/mol (DP 1,2) and 36,500 g/mol (DP 1,3) with a non-uniformity of about 2.

The calorimetric experiments were carried out with a Perkin-Elmer DSC 7 in N_2 atmosphere using the conditions indicated in the text. Before the real experiments were started, all the samples were heated up into the isotropic state to erase thermal history. The melting/crystallization transitions were identified by the maximum of the corresponding endothermal/exothermal peak. The glass transition temperature was taken at 1/2 of the step of the heat flow, respectively the heat capacity. Sample mass was usually close to 10 mg, the peak uncertainty was $\pm 0.5^{\circ}$C, the transition enthalpies were determined with standard software with an uncertainty of about ± 1 J/g.

RESULTS AND DISCUSSION

The structural variation of the polymers under consideration is given in Figure 1 and the corresponding standard calorimetric analysis is given in Figures 2–4.

Clearly at least 4 transitions can be detected in DP 1,1 (Figure 2): the glass transition at about 107°C, cold crystallization starting at about 160°C with its maximum at 178°C, melting to an anisotropic liquid of presumably smectic character, and the clearing point at 271°C. All give strong signals and the transitions are enantiotropic. The texture of the mesophase is unspecific but there is evidence from literature and preliminary X-ray analysis that a smectic mesophase is highly probable [17]. The cold crystallization vanishes after sufficient annealing at 160°C.

DP 1,2 mainly shows the glass transition, although a monotropic, anisotropic melt can be observed between crossed polarizers above 250°C, similarly in the DSC after long annealing under nitrogen. The texture is fine and rather unspecific with triangular patterns and

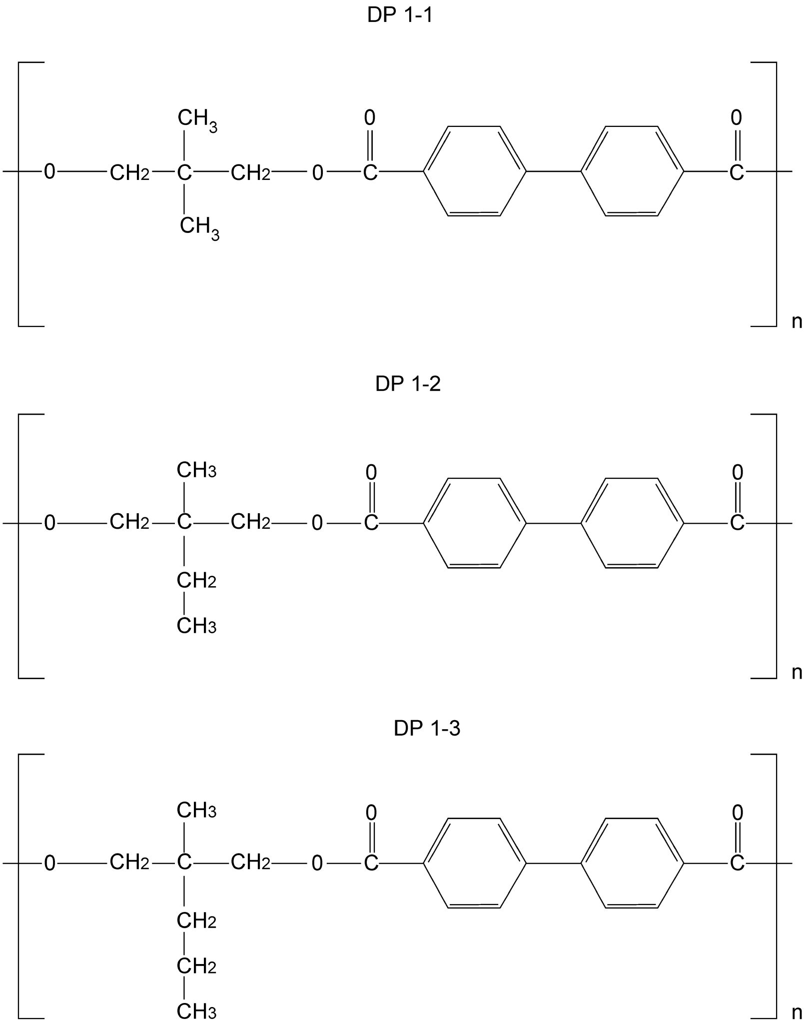

FIGURE 1 Structure of the poly[oxy(2,2′-dialkylpropane-1,3-diyl) carboxybisphenyl-4,4′-dicarbonyl] abbreviated DP 1,1; DP 1,2; and DP 1,3.

platelets. There are indications for a smectic structure from preliminary X-ray analysis. The glass transition temperature is at around 100°C. DP 1,3 shows results comparable with DP 1,2, the glass transition temperature is around 88°C. The tendency to form a crystalline or a mesophase phase decreases with growing length of the side-chain, and under ambient conditions these polymers can form isotropic,

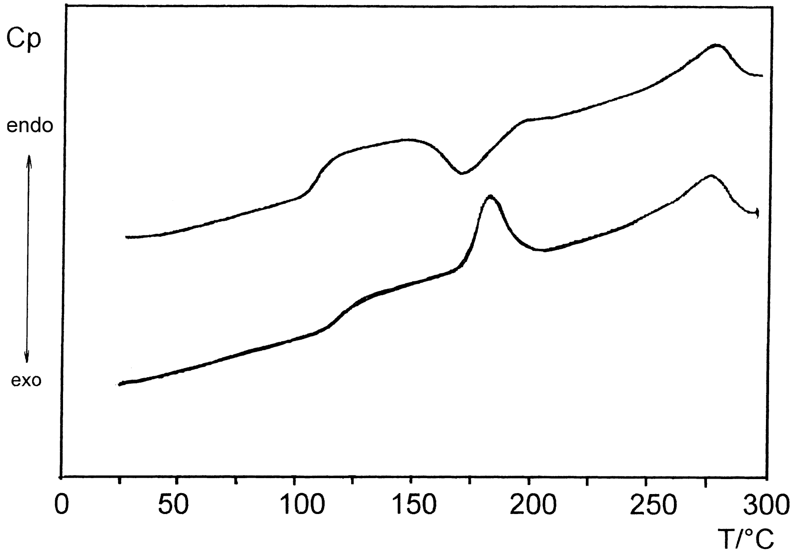

FIGURE 2 DSC-trace of DP 1,1 heating rate HR = 30 K/min. (Top) quenched sample, (bottom) after annealing 3 days at 160°C under N_2.

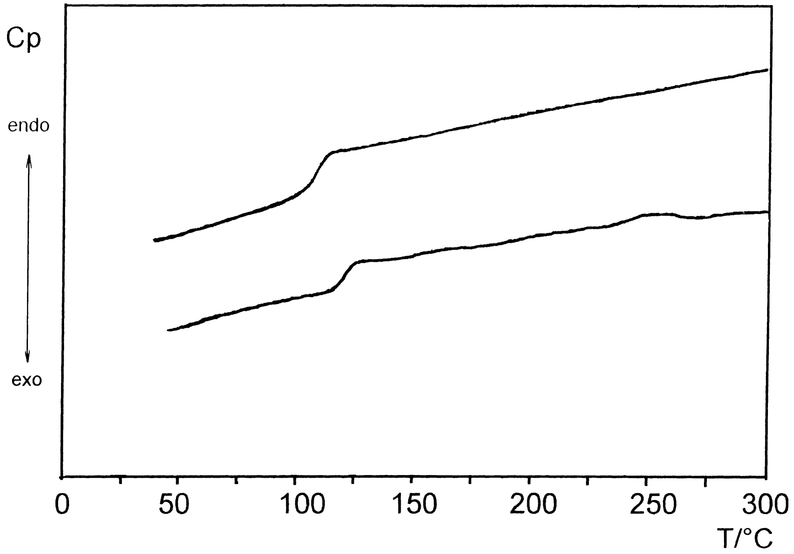

FIGURE 3 DSC-trace of DP 1,2 heating rate HR = 30 K/min. (Top) quenched sample, (bottom) after annealing 3 days at 160°C under N_2.

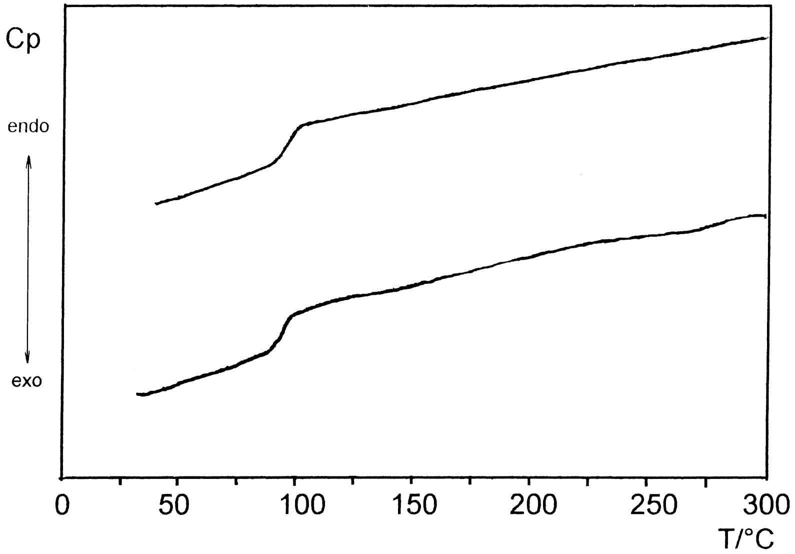

FIGURE 4 DSC-trace of DP 1,3 heating rate HR = 30 K/min. (Top) quenched sample, (bottom) after annealing 3 days at 160°C under N_2.

translucent glasses. Investigation of the behaviour of these materials dependence on pressure, volume and temperature (p-V-T), shows, however, unusual behaviour [18] and proves the monotropic behaviour of these two substances. Refractive index, expansivity and compressibility give them a potential for application in certain sensors [13].

The nature of the glass transition has been checked with respect to the validity of Ehrenfest's equations, and the results for DP 1,1; DP 1,2 and DP 1,3 are shown in Figures 5–7.

The differential coefficient dp/dT at the glass transition temperature was determined with p-υ-T-measurements as described elsewhere [13, 14] and is approximately a constant over the covered pressure range, as shown by the dotted line in Figures 5–7. Since we could measure c_p only at ambient pressure, only this value is indicated on the ordinate. The ordinate is given by f(p) plotting the product $\Delta\alpha/\Delta\kappa$ *vs.* the pressure p. According to Eqs. (5)–(7) all these values should match. However, there is always a large deviation between Ehrenfest's first (5) and second Eq. (6) so that there is always a large deviation from 1 in Eq. (7). Meixner [19] and Davie and Jones [20] showed that on introduction of more than one independent order parameter it is possible to describe deviations by an inequality instead of Eq. (7). However, *a priory* determination of its value is not possible and a more

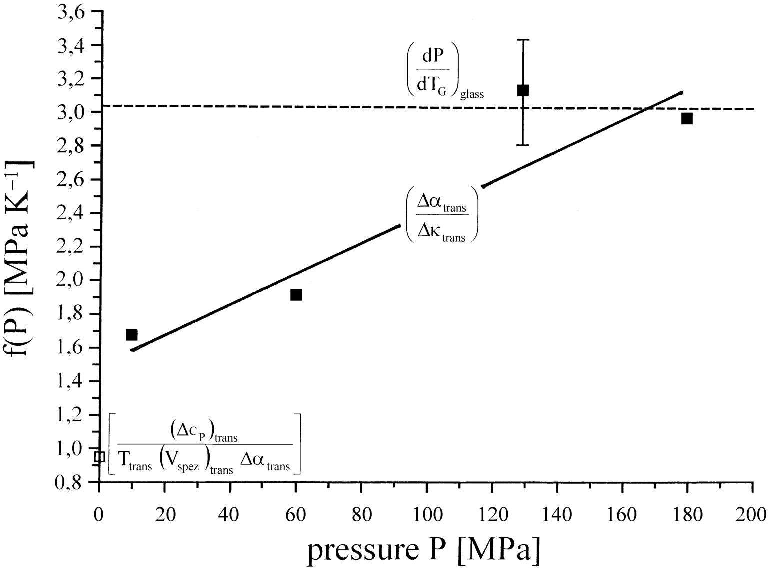

FIGURE 5 Ehrenfest's relations DP 1,1. For an explanation, see text.

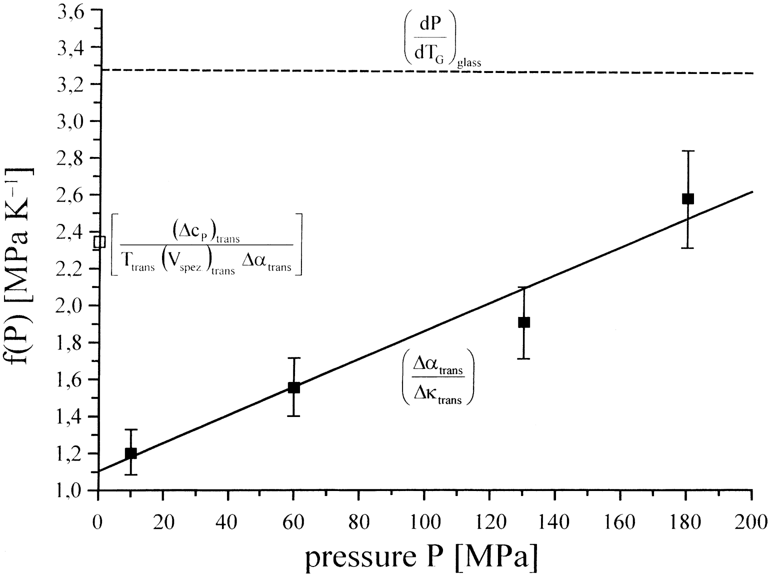

FIGURE 6 Ehrenfest's relations DP 1,2. For an explanation, see text.

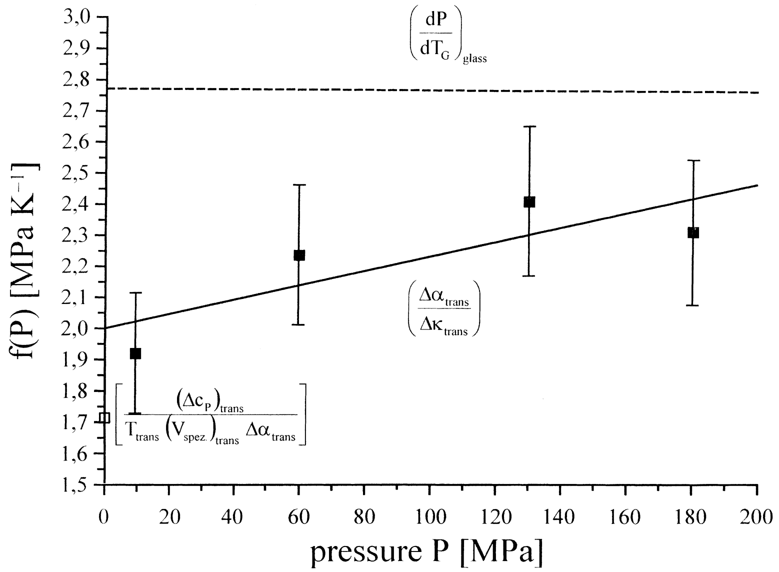

FIGURE 7 Ehrenfest's relations DP 1,3. For an explanation, see text.

accurate description requires a relation between those quantities which characterize the freezing-in temperature, such as viscosity or the different relaxation times, and the thermodynamic functions.

Since crystallization of DP 1,2 and DP 1,3 is restricted, an analysis of thermal behaviour beyond Tg could only be carried out regarding DP 1,1. There is always only one exothermal peak indicating crystallization between 200°C and 226°C depending on thermal history and heating rate. Heating of the samples show cold crystallization around 176°C and melting at 200°C–226°C. Annealing at different temperatures produces an additional melting peak around 167°C. A fast quenching from the melt followed by a sufficiently fast heating scan for the analysis (>30 K/min), shows no melting but only the isotropization at 278°C.

The thermal transitions are strongly influenced by the experimental conditions (cooling rate CR and heating rate HR an annealing time t_a at different annealing temperatures). Analysis of the thermal transitions after cooling down from the isotropic melt into the glass at different cooling rates (5°C/min, 10°C/min, 20°C/min and 50°C/min) shows an almost linear decrease of Tg with the cooling rate, ranging from 94,3°C (CR 50°min, HR 20°C/min) to 107,8°C (CR 50°C/min, HR 50°/min), while cold crystallization, melting into the mesophase and clearing point show a clearly non-linear dependence on the cooling rate as shown in Figure 8. While the clearing temperature is almost independent of HR, there is a clear heating rate dependence for all the other transitions caused by the well-known super-cooling effects.

We have investigated the influence of annealing temperatures and annealing time on the thermal transition. For this purpose samples were annealed up to 90 min at 130°C (that is at the beginning of the cold crystallization of a quenched sample), at 160°C (that is at the maximal rate of the cold crystallization) and at 190°C (that is close to the predominant melting maximum). After annealing, the samples were quenched with maximum cooling rate and analysed again. The results are shown in Figures 9–16.

Annealing at 130°C produces two crystalline populations, see Figure 9. The lower melting population (Tm ≅ 173°C) represents about 25% of the total crystalline material. It is growing only slowly with annealing time and requires about 20 min for the nucleation process. After about 100 min no further increase of the heat of fusion

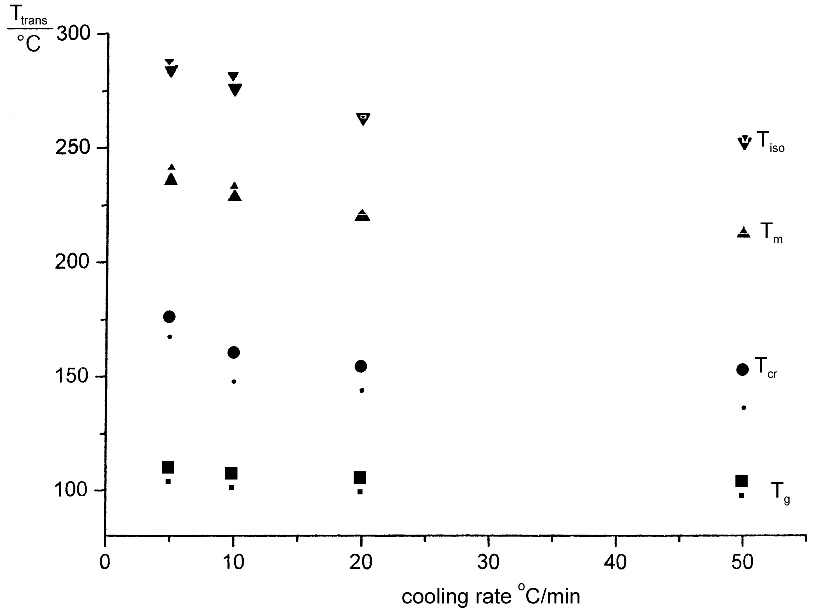

FIGURE 8 Dependence of the thermal transitions Tg, Tcr, Tm, and Tiso on the thermal history (cooling rate CR) and the analytical conditions (heating rate HR). Small symbols: HR 20°/min, large symbols: HR 50°/min.

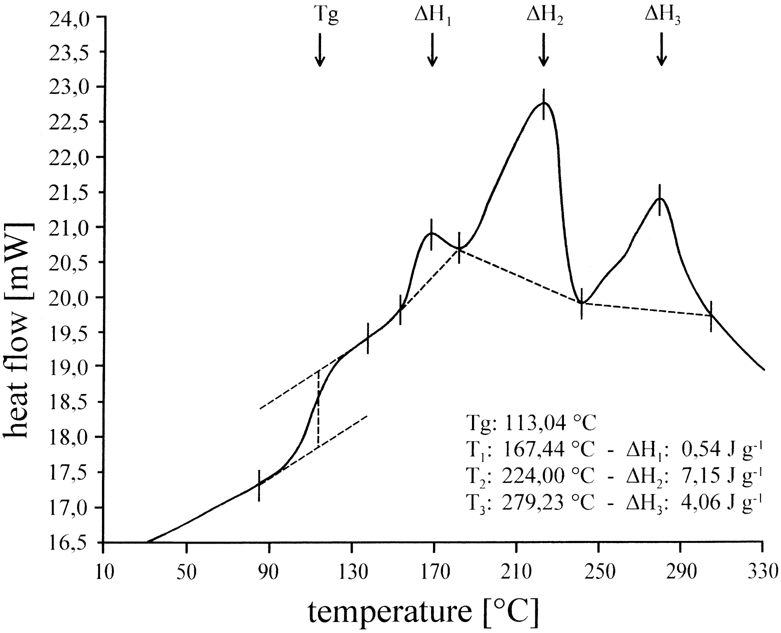

FIGURE 9 DSC-trace of DP 1,1 annealed for 20 min at 130°C, quenched and subsequently analysed with HR 50°C/min.

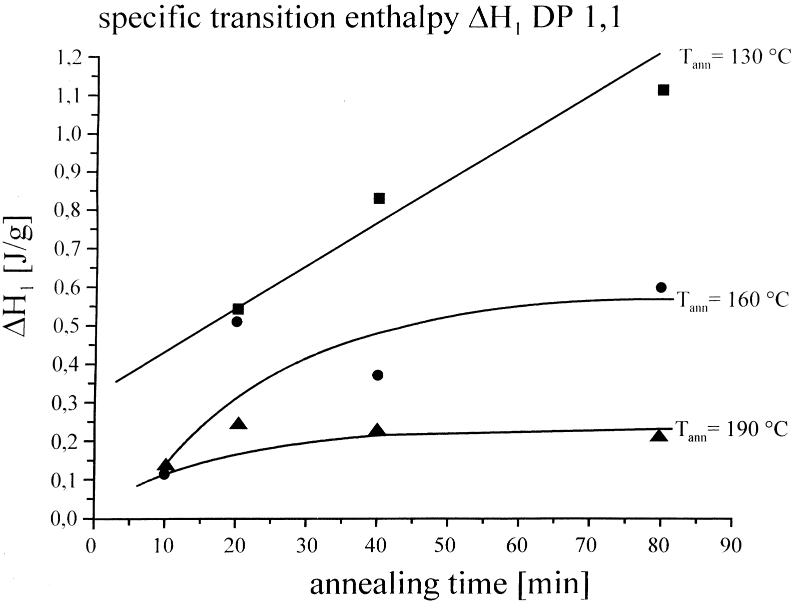

FIGURE 10 Enthalpy change of the low-temperature transition depending on annealing conditions.

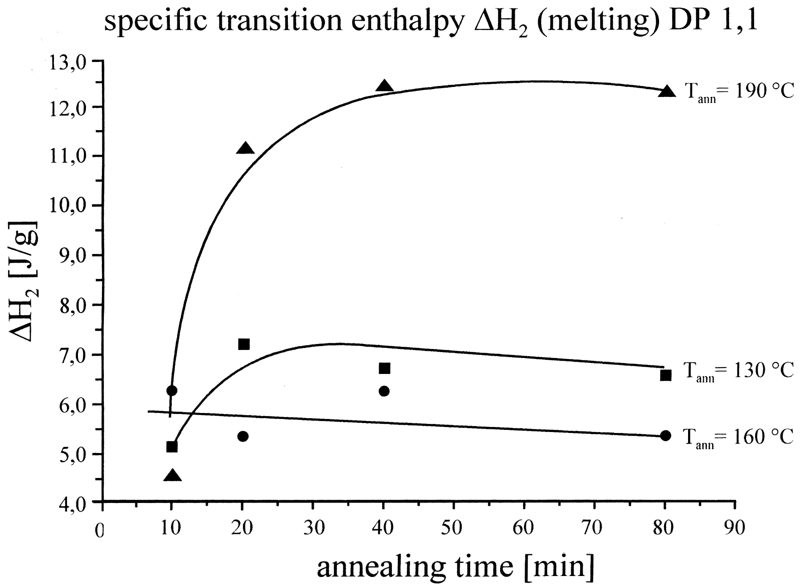

FIGURE 11 Enthalpy change of the main transition (melting to the liquid crystalline state) depending on annealing conditions.

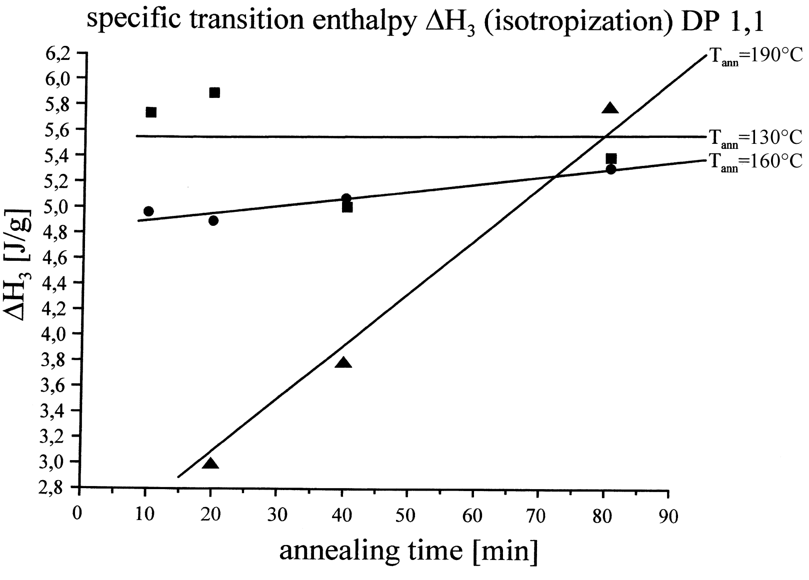

FIGURE 12 Enthalpy change of the isotropization depending on the annealing conditions.

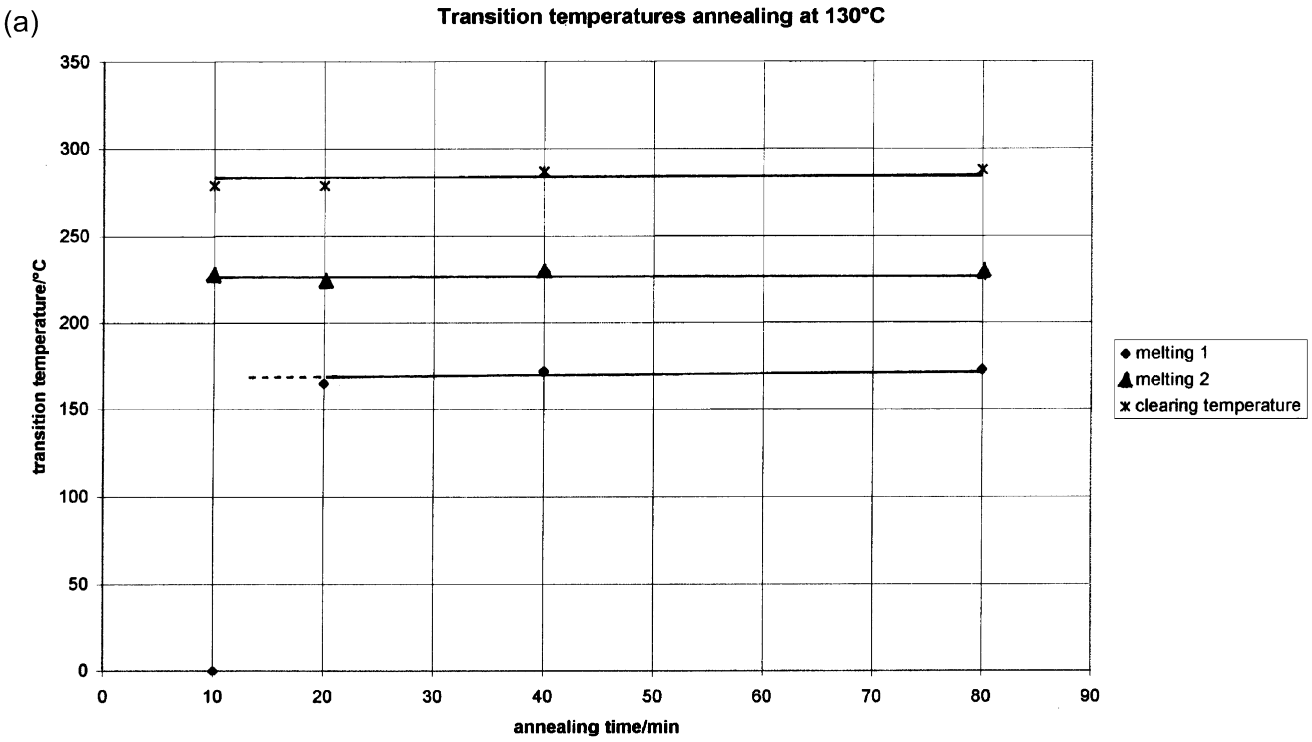

FIGURE 13 a) Dependence of the transition temperatures on the annealing time at 130°C. b) Dependence of the transition enthalpies on the annealing time at 130°C.

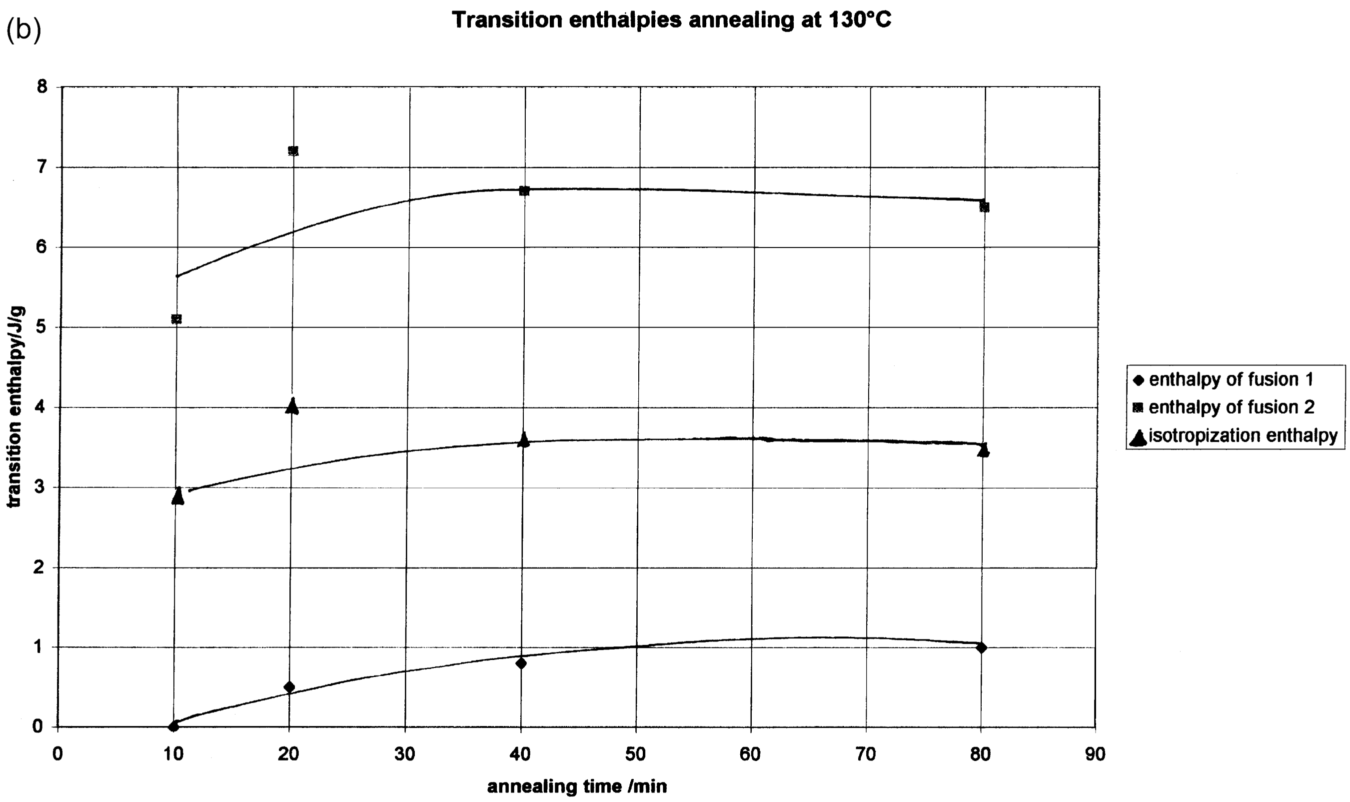

FIGURE 13 (*Continued.*)

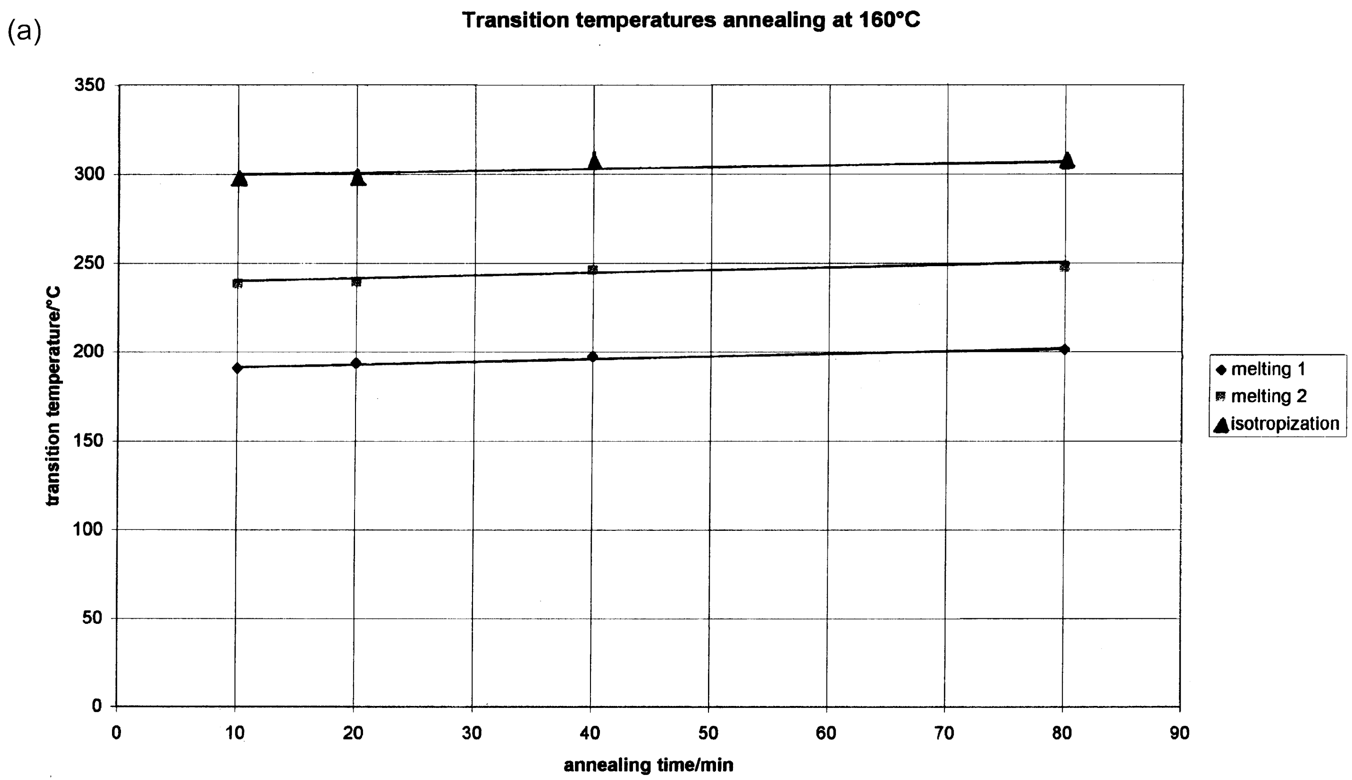

FIGURE 14 a) Dependence of the transition temperatures on the annealing time at 160°C. b) Dependence of the transition enthalpies on the annealing time at 160°C.

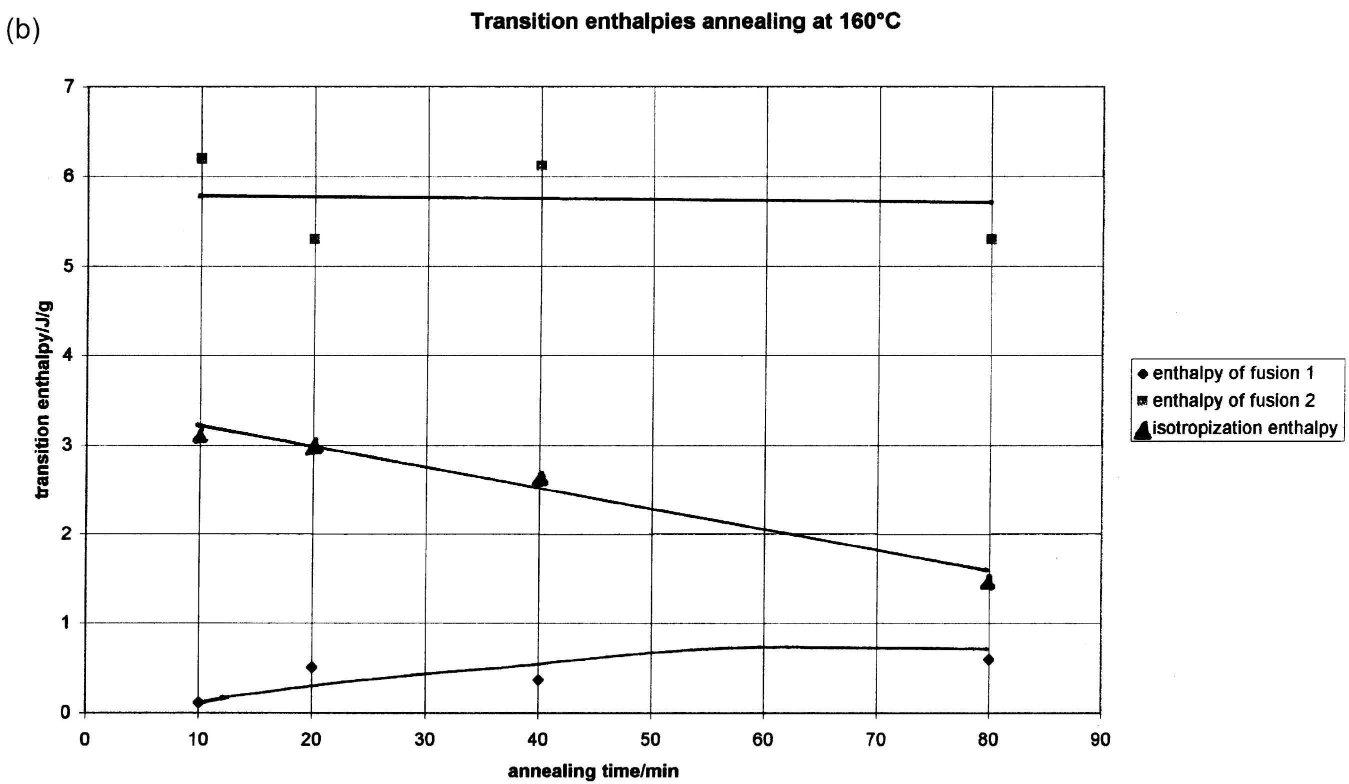

FIGURE 14 (*Continued.*)

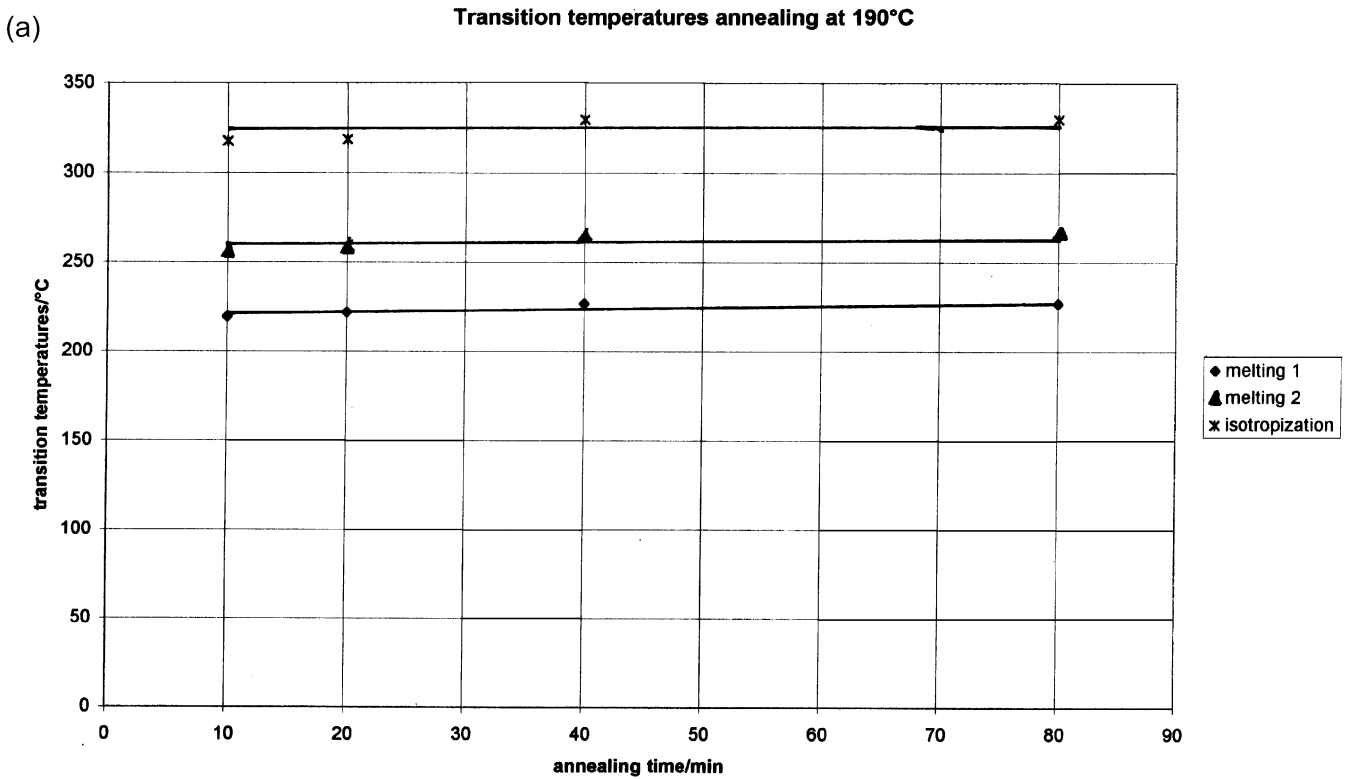

FIGURE 15 a) Dependence of the transition temperature on the annealing time at 190°C. b) Dependence of the transition enthalpies on the annealing time at 190°C.

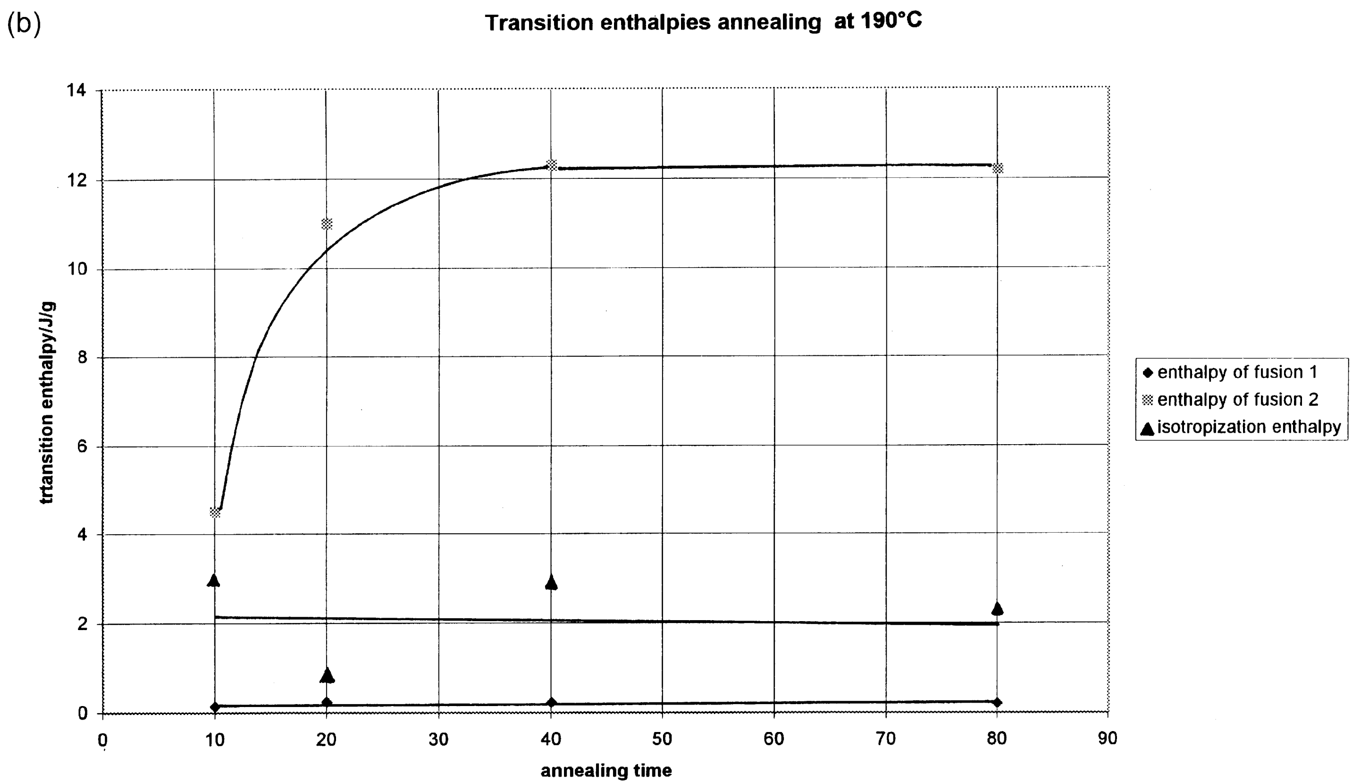

FIGURE 15 (*Continued.*)

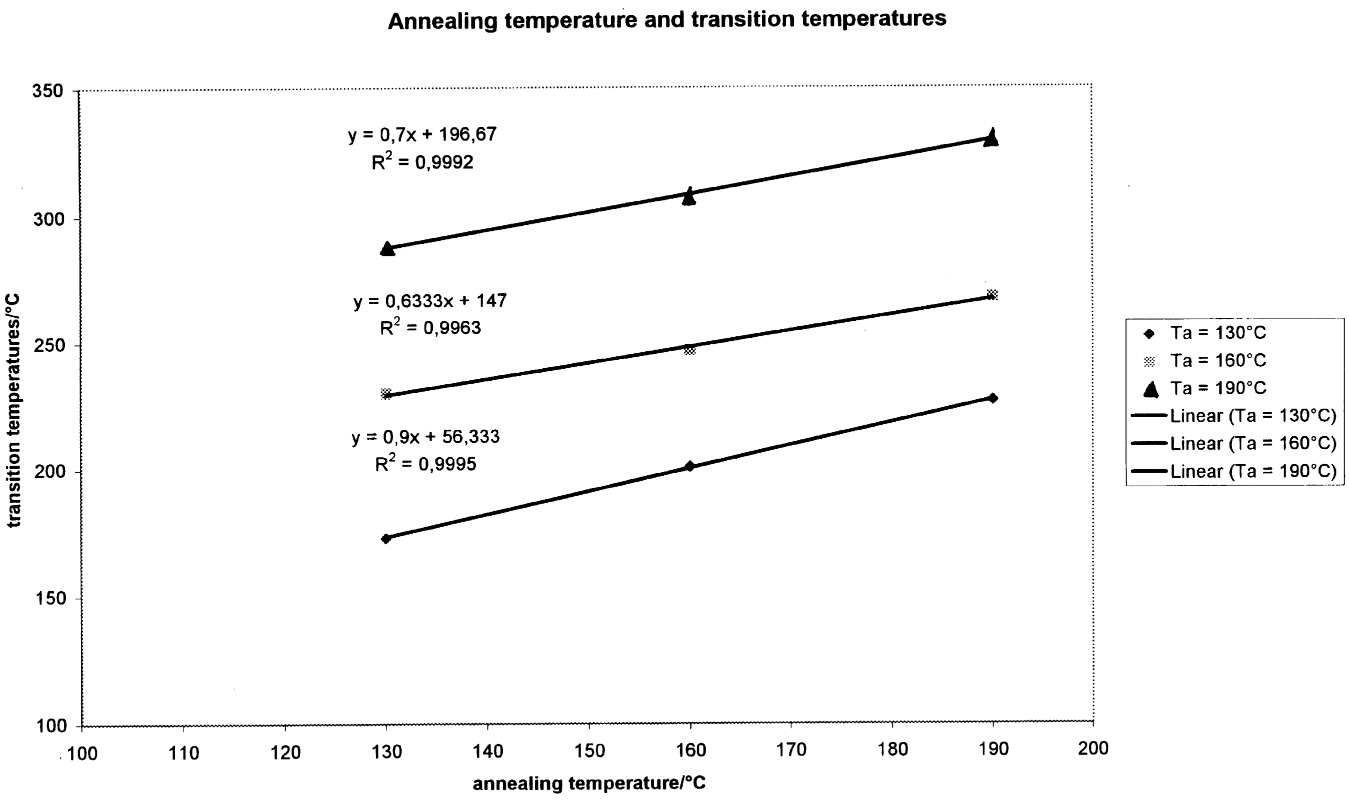

FIGURE 16 Dependence of the final transition temperatures on the annealing time and temperature.

(maximal value observed was 1 J/g) with annealing time was observed.

The strongest endothermal process (the transition into the liquid crystalline state at 230°C) is almost unaffected by annealing at 130°C. The same applies to the clearing temperature, $T_{iso} \cong 288°C$. The corresponding transition enthalpies increase almost parallel to each other, reaching a maximal value after about 20 min with a weak tendency to decrease with increasing annealing time. The corresponding enthalpies are around 6.5 J/g for the melting process and 3.5 J/g for the isotropization.

Annealing at 160°C, where the cold crystallization show its highest rate, leaves the transition temperatures almost independent of the annealing time, though with a slight increase during the first 40 min. In comparison with annealing at 130°C, the transition temperatures of the two developing crystalline populations are shifted to higher temperatures. The corresponding transition enthalpies are almost constant at about 0.5 J/g for the low temperature transition at about 200°C, 6 J/g for the 247°C endotherm, and finally 5 J/g for the isotropization at 308°C, although the values are at the limit of quantitative experimental accuracy, the effect is significant. While the transition enthalpy of the low-temperature transition reaches its maximum after about 20 min and remains there unaffected by further annealing, it was observed that the transition enthalpy of the main melting endotherm remains almost constant throughout the annealing time. The isotropization enthalpy increases slightly.

Annealing close to the maximum of the main endotherm at **190°C** shows a further increase of the transition temperatures: first endotherm at 227°C, main endotherm at 268°C, isotropization temperature at 330°C, being unaffected by the annealing time. The corresponding transition enthalpies are constant for the low temperature transition ($\cong$0.2 J/g). The main endotherm shows an increase of the melting enthalpy with annealing time. After about 30 min the maximum is reached with about 12 J/g. The isotropization shows a strong increase with annealing time and climbs during 80 min from 3 J/g to 5.6 J/g.

The higher the annealing temperature, the steeper the slope of the correlation between annealing temperature and annealing time. In general, the course of the isotropization follows the course of the melting of the main transition. On the other hand, the low-temperature transition shows the steepest slope of the annealing time-annealing temperature correlation at low temperatures. At higher annealing temperatures a rather early levelling out is observed, which is not observed on isotropization. The levelling out is also strong at the main transition but in this case it is pronounced at high annealing temperatures, close to the melting point. A possible explanation is that the low-temperature crystallization is fast after there are sufficient nuclei. Then what happens on annealing is mainly a re-organization of the structure to form more perfect crystals. The high-temperature crystallization, however, shows a stronger temperature dependence of crystallization. The isotropization, finally, goes parallel with the total amount of crystalline material.

It can be stated that annealing causes two different crystalline populations which form larger and/or more perfect crystals with increasing annealing temperature. There is a linear relation between the ultimate shift of the thermal transitions and the annealing temperature for all the first order transitions observed. The transition entropies of the ultimate transition temperatures after annealing are one order of magnitude smaller for the low-temperature endotherm and for the isotropization compared with the main melting process. Heating the samples at different heating rates influences the transition peaks in approximately the same way: smaller heating rates result in a higher transition enthalpy.

The results can be interpreted in the following way: There is a low-melting and a high melting component in DP 1,1 which crystallize independently of each other and which are not clearly resolved without annealing. The low-melting component cannot be interpreted as imperfect crystalline material already present in the sample which only forms more perfect crystals on annealing since the low-melting component occurs at the 130°C annealing temperature only after a certain annealing time. The melting points of both components shift to higher temperatures after annealing and the relative amounts of the two components seem to be constant within experimental error. The specific melting entropy at the transition temperature of the low-melting component is comparable to the isotropization entropy, indicating that this component probably has a lower symmetry compared with the higher melting crystallites and hence is probably closer to the mesophase than the high-melting crystalline material. The nature of the two different crystalline populations is still subject to investigation.

REFERENCES

[1] Hess, M. High Performance Polymers, In: Brostow, W. (Ed.) *Performance of Polymers*, Hanser Verlag, Mnchen, 2000.

[2] Lenz, R. W. (1985). *Faraday Disc. Chem. Soc.*, **79**, 21.

[3] Calundann, G. W. and Jaffe, M. (1982). *Proc. Robert A. Welch Found. Conf. Chem. Res.*, **26**, 247.

[4] Ballauff, M. and Schmidt, G. F. (1987). *Mol. Cryst.*, *Li. Cryst.*, **147**, 163.

[5] Hess, M. (1998). *Korean Polymer J.*, **6**(1), 1–27.

[6] Jonah, D., Brostow, W. and Hess, M. (1993). *Macromolecules*, **26**, 76–83.

[7] Blonsky, S., Brostow, W., Jonah, D. and Hess, M. (1993). *Macromolecules*, **26**, 84–88.

[8] Hess, M., Poersch, G. and Kosfeld, R. (1991). *Mat. Res. Soc. Symp. Proc.*, **183**, 123.

[9] Stickfort, L., Poersch, G., Hess, M. and Kosfeld, R. (1996). *J. Polym. Sci.*; *Polym. Chem.*, **34**, 1325–1330.

[10] Woelke, R. and Hess, M. (1999). *Polym. Eng. and Sci.*, **39**(3), 519–533.

[11] Baxmann, R., Hess, M., Veeman, W. S. and Woelke, R. (1999). *Macromol. Chem. Phys. Symp.*, **148**, 157–178.

[12] Saiter, A., Hess, M., Saiter, J. M. and Grenet, J., Macro 2000, Warsawa July, 2000, *Macromolecular Symp.*, to be published 2001.

[13] Woelke, R. (2001). *Ph.D. Thesis*, Duisburg, to be published 2001.

[14] Ehrenfest, P. (1933). *Proc. Kon. Akad. Wetensch. Amsterdam*, **36**, 153.

[15] Frenzel, J. and Rehage, G. (1980). *Macromol. Chem. Rapid Commun.*, **1**, 129.

[16] Rehage, G. and Borchard, W. (1973). In: Haward, R. N. (Ed.) *The Physics of the Glassy State*, *Appl. Sci. Publ.*, Barking, UK.

[17] Meurisse, P., Noel, C., Monnerie, L. and Fayolle, B. (1981). *Brit. Polym. J.*, **13**, 55.

[18] Hess, M., Woelke, R. and Pionteck, J., *Macro. Res. Innov.*, submitted (2000).

[19] Meixner, J. (1952). Changement de Phases, Paris, p. 432.

[20] Davies, R. O. and Jones, G. O. (1953). *Proc. Roy. Soc.*, **217A**, 26.